Investigation of roughness induced crack closure effects in fatigue

M.R. Parry, S. Syngellakis & I. Sinclair
School of Engineering Sciences, University of Southampton, Southampton, SO17 1BJ, UK.

Abstract

The incidence of roughness induced fatigue crack closure has been studied by finite element modelling. Results show an increasing effect of crack path angle on closure levels with the closure mechanism being strongly dependent on residual plastic strains in the wake rather than global shear displacements of the fracture surfaces. An analytical expression for the functional dependence of roughness induced closure has been produced which shows reasonable agreement with the finite element results.

1 Introduction

The phenomenon of fatigue crack closure is widely considered to have a strong influence on fatigue crack growth. As such, directed alloy development, accurate life prediction and the implementation of economic inspection procedures in engineering structures are dependent upon the ability to quantify this effect [1, 2]. Many aluminium aerospace alloys exhibit microscopically deflected crack growth modes, with various aspects of fatigue crack growth then being rationalised by the associated incidence of roughness induced crack closure (RICC) [3]. Whilst numerous experimental studies and modelling exercises on crack closure have been reported over the last 30 years, significant controversy remains. For example, Vasudevan and co-workers [4, 5] have suggested that the actual influences of closure on crack growth are dramatically lower than many works in the literature suggest. An extensive body of experimental evidence and theoretical analysis does however exist to support the dependence of fatigue crack growth on closure phenomena. Several quantitative and semi-quantitative models of RICC exist within the literature, although they are generally rather simplified. Furthermore, interactions between different

closure mechanisms are largely ignored. The present work seeks to extend current quantitative understanding, focusing on geometrical and micromechanical closure effects for a propagating crack in an elasto-plastic material.

1.1 Background

The discovery of *extrinsic* contributions to fatigue crack growth resistance is usually attributed to Elber [6]. Elber noted that as a fatigue crack propagates, plastically stretched material in the crack wake leads to premature contact of the crack faces, a process referred to as plasticity induced crack closure (PICC). Other mechanisms by which shielding of a crack tip can occur have since been identified (e.g. see [7]). The possibility that crack path roughness may lead to premature crack closure was first identified by Walker and Beevers [8], who noted that in the apparent absence of PICC, contact occurred at discrete points behind the crack tip as a result of deflected crack growth and an associated shear of the crack flanks. In order for RICC to occur a combination of crack path deflection and a residual shear offset of the fracture surfaces is clearly required. The origin of this residual offset has commonly been ascribed to irreversible deformation ahead of the mixed-mode crack tip [9]. Whilst PICC is generally considered to be most pronounced under plane stress conditions, high levels of crack closure have been reported for plane strain, near threshold conditions [9]. Such results have been related to high levels of RICC due to extensive deflected crack growth in the near threshold regime.

1.2 Finite element modelling of PICC

A finite element (FE) model of PICC was presented by Newman and Armen [10], which predicted crack face contact under tensile far field loads in general agreement with experimental observations. Similar models have subsequently been used by many researchers to investigate closure under different stress states and loading conditions [e.g. see 11]. A detailed review of the important issues (mesh sufficiency etc.) in FE modelling of closure is presented by McClung and Sehitoglu [11]. Various issues regarding the definition of the crack closure point in a plane strain FE analysis have also be identified [12]. A fuller discussion on these points is presented elsewhere [13].

1.3 RICC specific models

Suresh and Ritchie [14] have derived an expression for the closure stress intensity factor K_{cl}/K_{max} due to RICC as a function of crack deflection angle, using a simple geometrical model. In this work the mode II offset was essentially arbitrary, but was assumed to come from irreversible plastic deformation at the crack tip. Llorca [15] has used the finite difference technique, in a manner similar to the FE models of Newman and Armen, to demonstrate the effect of periodic and irregular crack deflections on closure for low ΔK plane

strain conditions. It was shown that increasing levels of crack closure occur with increasing crack deflection angle, which are further enhanced by varying deflection angle along a given crack path. As noted earlier, for crack roughness to enhance closure levels, some residual shear offset of the fracture surfaces must exist. The only source of this offset can be plasticity effects, however these do not appear to be accurately addressed in Llorca's work.

1.4 Scope and objectives of the present work

The present work is concerned with the finite element modelling of crack closure, arising from the combined effects of crack deflection and prior plastic deformation, in a long fatigue crack in an aerospace aluminium alloy under constant amplitude cyclic loading such that small scale yielding conditions exist at the crack tip. This has been done through an extension of the fatigue crack growth modelling concepts of Newman and Armen [10] to the case of a periodically deflected crack. Continuum plasticity theory has been used with attention being paid to accurate modelling of crack tip plasticity in line with McClung and Sehitoglu's recommendations [11]. The underlying mechanism leading to the observed RICC has been identified through the isolation of the effects of deflected crack propagation and the effects of plastic deformation at the crack tip.

2 Development of the finite element models

The general purpose finite element code ABAQUS [16] was used to model a standard centre cracked plate specimen of width $W = 75$mm, initial crack length $a_0 = 7.6$mm, thickness $B = 7.5$mm. Symmetry considerations allowed one half of the specimen to be modelled for deflected crack growth (one quarter for the undeflected crack models). Material properties analogous to a damage tolerant aluminium alloy were chosen. i.e. yield stress $\sigma_0 = 370$ MPa, Young's modulus $E = 74$ GPa, hardening modulus $H = 0.07E$, Poisson's ratio $\nu = 0.3$. These were implemented in a standard linear kinematic hardening model. Approximately 10000 4-node quadrilateral elements were used to discretise one half of the CCP specimen (5000 elements in the quarter model). The mesh was designed such that the element dimension, L_e, along the crack line was 1μm, with the crack allowed to grow up to 100 μm. McClung and Sehitoglu's criterion [11] for mesh sufficiency requires that $L_e \leq 0.1r_p$ where r_p, is the forward plastic zone size at maximum load. This requirement means that the adopted L_e is acceptable for a minimum r_p of 10 μm. In order to obtain stabilised crack closure, experimental results [17] suggest that the crack should be allowed to grow through the equivalent of four plastic zone sizes, giving a maximum r_p of 25 μm. Under plane strain conditions this range of r_p (from 10 μm to 25 μm) equates to $\Delta K = 3.6 - 5.7$ MPa$\sqrt{m}$ which corresponds to the near threshold fatigue regime in which RICC processes are prominent. Five different crack geometries were modelled; an undeflected crack, and cracks undergoing periodic deflections of 15°, 30°, 45° and 60°.

A procedure for incremental crack propagation was developed along the lines of Newman's work [10, 12]. Pairs of opposite nodes along the crack line were initially connected by two (very short) linear spring elements. The first spring element had no stiffness in compression but was very stiff in tension. The second spring element was very stiff in compression, but had no stiffness in tension, with the spring stiffness acting normal to the crack face so as to prevent crack face interpenetration without affecting the relative shear displacement of the crack faces. Crack propagation was simulated by removing the tension spring element at the crack tip node at maximum load. This allowed the crack to grow one element dimension as the original crack tip nodes were no longer constrained in tension. To assess the role of plastic deformation on the RICC process, modelling was also carried out on a non-propagating deflected crack, and a deflected crack propagated in single jumps between each crack turning point. Friction effects during contact of the crack surfaces were not considered here.

3 Results and discussion

3.1 Finite element results

The effect of periodic crack deflection on K_{cl}/K_{max} under plane strain loading at ΔK = 4.63 MPa m$^{1/2}$ can be seen from the plot of the deformed mesh of a 45° deflected crack at $K < K_{cl}$ in Figure 1. Closure can be seen to have occurred at discrete points near the asperity tips, with the bulk of the crack remaining open, as noted by Walker and Beevers [8].

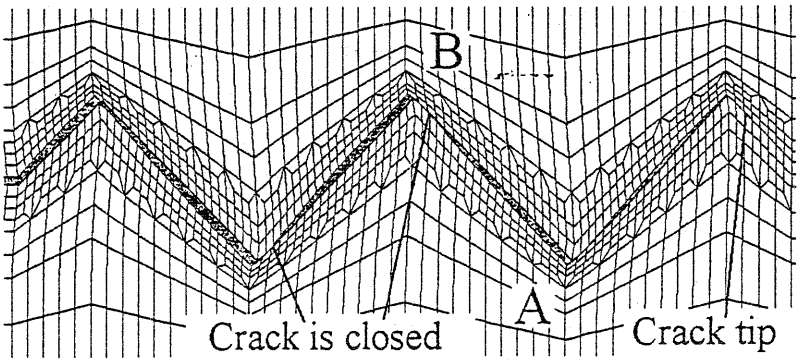

Figure 1: Deformed mesh of 45° deflected crack exhibiting RICC.

From Figure 2, it is evident that the closure levels increase strongly with deflection angle, with the closure point defined by first asperity contact behind the crack tip, as discussed in [13]. It appears that quasi-stabilised levels of closure are reached when the crack has propagated through the first two deflections. The closure levels are at a maximum shortly after a deflection, and then drop off steadily as the crack tip moves away from the point of deflection.

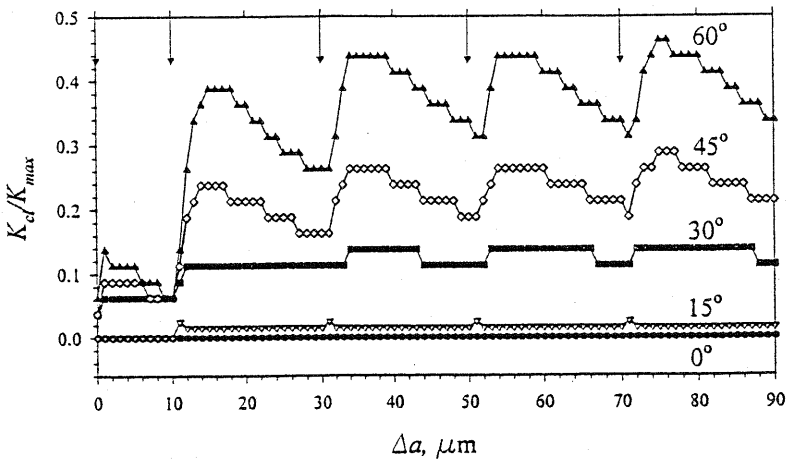

Figure 2: Crack closure levels for varying deflection angles. Arrows indicate position of deflections.

An important observation from these results is the sense of the shear displacements giving rise to asperity contact. In particular it may be seen that the direction of the relative displacements of the upper and lower fracture surfaces at each asperity tip changes along the crack wake. At point 'A' in Figure 1 the lower fracture surface is displaced away from the crack tip (in relation to the upper fracture surface), whilst at point 'B' it is displaced towards the crack tip. It may then be seen that the shear displacements giving rise to closure along the crack wake cannot be 'global' displacements of the upper and lower fracture surfaces due to mixed mode behaviour at the active crack tip. The asperity shear displacements in Figure 1 can in fact only arise from local residual strains from the crack propagation process. The asperity displacements and contacts observed in the present models are therefore somewhat different to the conventional representation of RICC. Indeed, the conventional description of RICC due to global fracture surface offsets arising from mixed-mode crack tip plasticity is questionable. Firstly, under small scale yielding conditions, the crack tip plasticity will present a local perturbation to the displacement field. Away from the immediate crack tip zone the effect of the residual plastic deformation at the tip on the fracture surface displacement will be minimal. Secondly, a fatigue crack does not necessarily exhibit a common deflection angle through the specimen thickness. Along the crack front, the crack may be deflected above and below the nominal mode I crack growth direction. Hence the average deflection angle along the crack front, and hence the averaged contribution to global shear of the fracture surfaces will be approximately zero.

The behaviour of the present models may be rationalised as follows: when a simple deflected crack tip is loaded as shown in Figure 3(a), a permanent plastic shear deformation is produced in the direction/sense shown. On unloading, a degree of reverse plasticity will occur, although a net residual deformation will remain in the direction of the original loading. As such, the crack tip will held in

a 'compressive' shear (of opposite sense to the loading shear) by the surrounding elastic material when unloading occurs, exactly analogous to the compressive load generated by crack tip plasticity when a simple mode I crack is unloaded. When turning of the crack occurs, as shown in Figure 3(b), this residual plastic strain/compressive loading will always promote closure on the forward edge of each asperity tip, as seen in Figure 1. To illustrate the above process, various simplified models were investigated. Figure 4(a) illustrates the unloaded condition of a deflected crack where the crack path was simply 'cut' without a propagation process, with the crack then being loaded and unloaded once, with the resultant plastic deformation producing a degree of shear offset along the asperities. The shear is of identical direction for all asperities, consistent with deformation at the tip being the only source of shear offset, but is in fact insufficient for closure to occur due to the associated residual tensile opening (displacements are greatly magnified in the diagram).

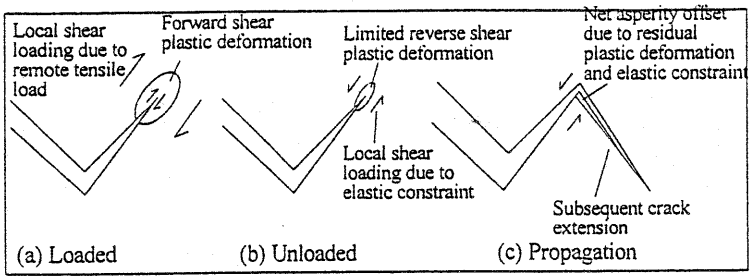

Figure 3: Crack closure due to residual shear deformation in the wake.

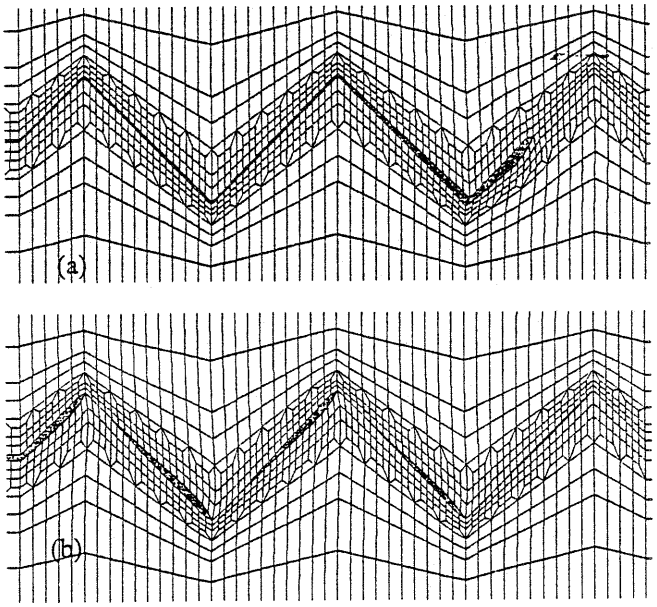

Figure 4: Deformation due to (a) pure tip, and (b) pure wake effects.

In Figure 4(b) the crack has been propagated with loading and unloading only being applied at each crack turning point. For the final crack length shown the crack is simply loaded and unloaded elastically, i.e. no shear offset can be generated at the tip. Closure behaviour is seen to be closely analogous to that in Figure 1, confirming the role of residual plastic shear displacements along the crack wake in producing closure. This dependence of RICC on residual displacements in the crack wake has also been identified experimentally [18]. It may be seen that the predominant closure process is in fact closely analogous to plasticity induced closure in mode I loading, although it does rely on crack path roughness to generate the necessary shear displacements. It is important to note that plane stress conditions are not particularly necessary to the asperity contact process shown in Figure 3 (i.e. as generally recognised for simple mode I plasticity induced closure), as the critical deformations are shear in nature and do not require through-thickness contraction for volume conservation.

3.2 Analytical RICC model

By considering the geometry of the deflected crack it is possible to predict the functional dependence of RICC due to the mechanism described in the previous section. Consider Figure 5, which shows a point of crack deflection. A residual shear h exists at the asperity tip due to previous plastic deformation. For an asperity which is sufficiently distant from the crack tip, crack opening near the asperity tip may be estimated from elastic behaviour. Considering local mode I loading as the primary source of crack opening, then the crack flank displacement at maximum load, δ_{max}, at the asperity tip is given by [19],

$$\delta_{max} = \frac{4\,V\,k_{I\,max}\left(1-\nu^2\right)\sqrt{\Delta a}}{F\sqrt{\pi}\,E}, \qquad (1)$$

where Δa is the distance from the crack tip to the first asperity, V and F are geometry correction factors (V=1.46, F=1.122 for small a), and k_{Imax} is the local

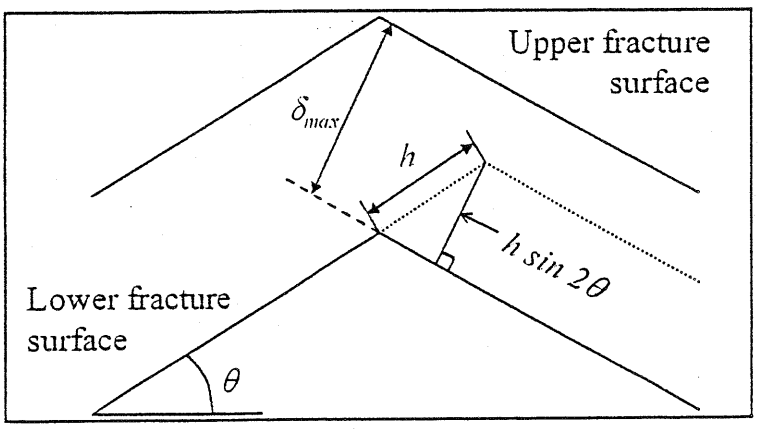

Figure 5: Geometry of crack deflection model.

maximum mode I stress intensity factor. From Figure 5 the component of h normal to the crack face is given by $h \sin 2\theta$, and given that $\delta \propto K$ (i.e. elastic behaviour), we have,

$$\frac{K_{cl}}{K_{max}} = \frac{h \sin 2\theta}{\delta_{max}}. \tag{2}$$

The value of h may be expected to scale with local mode II opening of the tip prior to crack turning (for a fixed R-ratio). As such h may be given by,

$$h = \frac{\beta k_{2max}^{2}}{\sigma_0 E}. \tag{3}$$

where β is a constant, and k_{2max} is the local maximum mode II stress intensity factor. Hence from eqns 1-3,

$$\frac{K_{cl}}{K_{max}} = \frac{\beta F \sqrt{\pi} k_{2max} \sin 2\theta}{4V\left(1-\nu^2\right)\sigma_0 k_{1max}\sqrt{\Delta a}}. \tag{4}$$

From linear elastic analysis [20], the local mode 1 and 2 stress intensity factors at the tip of a deflected crack are,

$$\begin{aligned} k_{1max} &= \tfrac{1}{4}\left(3\cos\tfrac{\theta}{2} + \cos\tfrac{3\theta}{2}\right)K_{1max} \\ k_{2max} &= \tfrac{1}{4}\left(\sin\tfrac{\theta}{2} + \sin\tfrac{3\theta}{2}\right)K_{1max} \end{aligned}, \tag{5}$$

where K_{1max} is the maximum mode I stress intensity factor for a straight crack of equal length. Combining eqns 4 and 5 gives,

$$\frac{K_{cl}}{K_{max}} = \frac{\beta F \sqrt{\pi} K_{1max}\left(\sin\frac{\theta}{2} + \sin\frac{3\theta}{2}\right)^2 \sin 2\theta}{16V\left(1-\nu^2\right)\sigma_0\sqrt{\Delta a}\left(3\cos\frac{\theta}{2} + \cos\frac{3\theta}{2}\right)}. \tag{6}$$

The predicted angular dependence of RICC is plotted in Figure 6, for $\beta = 1.5$, and $\Delta a = 8\mu m$, for which closure levels are at their maximum in the FE model, and $\Delta a = 20\ \mu m$, for which they are at a minimum.

The agreement between the analytical expression and the FE results is excellent. The value of β was evaluated from the FE models and was found to be in the range 1.7 - 2.8, i.e. in reasonable agreement with the value of 1.5 used in Figure 6 given the simplicity of the analytical model. Furthermore, it should be noted that the angular functionality of the analytical expression is not influenced by the β value.

The variation of K_{cl}/K_{max} with increasing crack length is illustrated in Figure 7 for the 60° deflected crack. It can be seen that as the crack tip just passes a deflection (i.e. Δa is very small) eqn. 6 significantly over-predicts the value of K_{cl}/K_{max}. However for larger Δa the two solutions agree well. The over-prediction of K_{cl}/K_{max} at very small Δa can be accounted for by more predominant plastic blunting effects near the tip. It is interesting to note that eqn 6 predicts that K_{cl}/K_{max} should increase monotonically with K_{max} for fixed R, counter to experimental observations. However it is important to realise that the region over which the plastic crack tip blunting effects will dominate may be expected to scale with K_{max}^2.

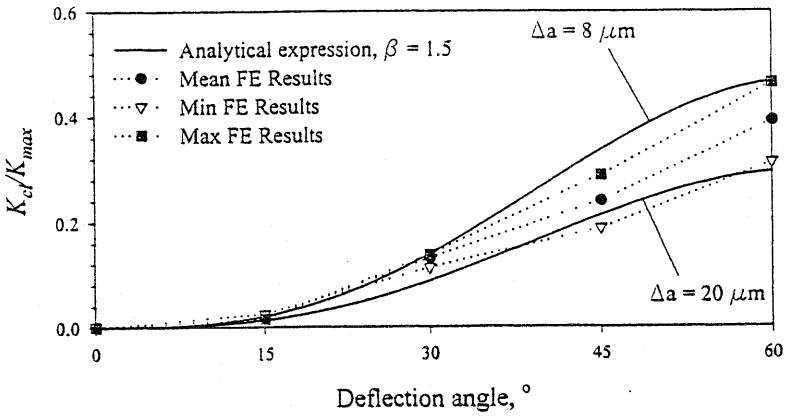

Figure 6: Angular dependence of RICC.

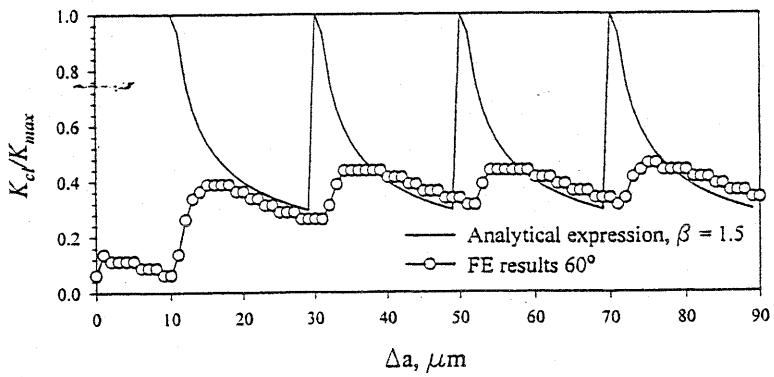

Figure 7: Crack length dependence of RICC

4 Conclusions

1. Existing finite element techniques have been extended to investigate crack closure arising from crack deflection and plasticity.
2. Periodic crack deflection has been shown to significantly increase crack closure levels in plane strain, with the effect increasing with deflection angle.
3. The closure mechanism has been shown to be due to the local residual strains arising from the crack propagation process, rather than 'global' shear displacements due to mixed-mode behaviour at the crack tip.
4. An analytical expression for RICC has been produced which predicts a dependence on crack deflection angle and crack length in reasonable agreement with the FE results.

References

[1] Saxena, V.K., Radhakrishnan, V.M. *Mater. Sci. Tech.*, **14**, pp. 1227-1241, 1998.

[2] Newman Jr, J.C. Engineering Against Fatigue, Sheffield, UK, March 17-21, 1997, A.A.Balkema, Rotterdam, 1999, pp. 261-268.

[3] Venkateswara Rao, K.T. & Ritchie, R.O. *Int. Mater. Rev.*, **37**, pp. 153-185, 1992.

[4] Vasudevan, A.K., Sadananda, K. & Louat, N., *Scripta Metall. Mater.*, **27**, pp. 1673-1678, 1992.

[5] Louat, N., Sadananda, K., Duesbury, M. & Vasudevan, A.K. *Metall. Trans.*, **24A**, pp. 2225-2232. 1993.

[6] Elber, W. *Engng. Fract. Mech.*, **2**, pp. 37-45, 1970.

[7] Ritchie, R.O. *Mater. Sci. Engng.*, **A103**, pp.15-28, 1988.

[8] Walker, N. & Beevers, C.J. *Fatigue Engng. Mater. Struct.*, **1**, pp. 135-148, 1979.

[9] Minakawa, K. & McEvily, A.J. *Scripta Metall.*, **15**, pp. 633-636, 1981.

[10] Newman Jr., J.C. & Armen, H. *AIAA J.*, **13**, pp. 1017-1023, 1975.

[11] McClung, R.C. & Sehitoglu, H. *Engng. Fract. Mech.*, **33**, pp. 237-252, 1989.

[12] Fleck, N.A. & Newman Jr., J.C., *Mechanics of Fatigue Crack Closure*, ASTM STP 982, American Society for Testing and Materials, Philadelphia, U.S.A., pp. 319-341, 1988.

[13] Parry, M.R., Syngellakis, S. & Sinclair, I. *Mater. Sci. Engng.*, in press, 1999.

[14] Suresh, S. & Ritchie, R.O. *Metall. Trans.*, **13A**, pp. 1627-1631, 1982.

[15] Llorca, J. *Fatigue Fract. Engng. Mater. Struct.*, **15**, pp. 655-669, 1992.

[16] ABAQUS v5.8, Hibbitt, Karlsson & Sorensen, Inc., Rhode Island, U.S.A., 1998.

[17] Ward-Close, C.M. & Ritchie, R.O. *Mechanics of Fatigue Crack Closure*, ASTM STP 982, American Society for Testing and Materials, Philadelphia, U.S.A., pp. 93-99, 1988.

[18] Fitzpatrick, M.E., Bhattacharjee, D., Cree, A.M. & Daykin, C.R.S. *Scripta Mater.*, **35**, pp. 1335-1340, 1996.

[19] Tada, H., Paris, P.C. & Irwin, G.R. *Stress Analysis of Cracks Handbook*, Del Research Corporation, Hellertown, 1973.

[20] Bilby, B.A., Cardew, G.E. & Howard, I.C. *Fracture 1977*, **3**, pp 197-200, 1977.

Damage and Fracture Mechanics VI

Computer Aided Assessment and Control

EDITORS:

A.P.S. Selvadurai
McGill University, Canada

C.A. Brebbia
Wessex Institute of Technology, UK

WIT PRESS Southampton, Boston

Damage and Fracture Mechanics VI

Computer Aided Assessment and Control

A.P.S. Selvadurai
C.A. Brebbia
Editors

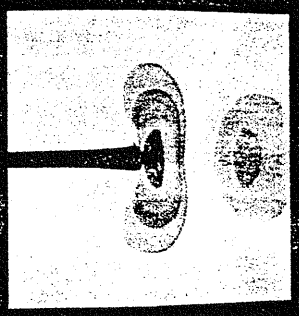

WIT PRESS